HEFAT2014
10th International Conference on Heat Transfer, Fluid Mechanics and Thermodynamics
14 – 16 July 2014
Orlando, Florida

FINITE ELEMENT MODELING OF STRUCTURAL DESIGN OPTIMIZATION OF VARIOUS VERTICAL AXIS WIND TURBINE MODELS

Rahman M.*, Smith A., Freeman A., Denham J., Christopher L., Huggins W., Johnson Z., and Ragland J.
*Author for correspondence
Department of Mechanical Engineering,
Georgia Southern University,
Statesboro, Georgia, 30460,
USA,
E-mail: mrahman@georgiasouthern.edu

ABSTRACT

Wind is among the most popular and fastest growing sources of alternative energy in the world. It is an inexhaustible, indigenous resource, pollution-free, and available almost any time of the day, especially in coastal regions. Vertical axis wind turbines (VAWTs) are more practical, simpler, and significantly cheaper to build and maintain than horizontal axis wind turbines (HAWTs). They have other inherent advantages; for example, they always face the wind; can run at low wind speed without any starting torque. As well, they may even be critical to mitigating the grid interconnection stability and reliability problems that currently face electricity producers and suppliers. Cheap VAWTs may provide an alternative to destroying rainforests to grow biofuel crops.

The purpose of this study is to perform a finite element static stress analysis to develop structurally stable and relatively efficient vertical axis wind turbine (VAWT) model design. VAWTs are typically used for lower wind speeds as opposed to HAWTs which are used in commercial wind farms that are used to produce a high energy output. For the finite element simulation, three different VAWT models such as conventional Savonius rotor, Helical Savonius rotor, and the Giromill type VAWT were considered. For the first two types VAWTs, rotation occurs due to the drag force generated due to the pressure difference between the concave and convex surfaces of the turbine blades. Whereas for the Darrieus rotor or Giromill type VAWT, rotation occur due to the lift force generated by the wind blowing past the airfoil shaped blades. The ANSYS FLUENT, a finite element based computational fluid dynamics solver, is adopted to obtain the pressure distributions on the Savonius type models and the lift force for the Giromill model. Each of the VAWTs is tested in ANSYS static structural modeler with three different types of materials such as aluminum alloy, stainless steel, and PVC. Also the Giromill turbine model is tested using two different types of airfoils that have two different lift coefficients. Comparison of the symmetric NACA 0012 and NACA 0714 airfoils of unit chord were chosen for the analysis of the Giromill model design. In this analysis, the airfoils were not allowed to move and the pitch angle of airfoil was assigned to the air flow at the inlet boundary of the domain. The goal of the numerical simulation was to determine the location and magnitude of maximum equivalent stress and total deformation of the blades of each model to determine the structural stability improvement and efficient design of the VAWT models. In all cases, the stainless steel made model deformed the least while aluminum model had a few more in deformation and PVC model experienced the highest amount of deformation. This was expected because PVC was the lightest of all the materials used in this study. The stresses were about the same for each case except for the NACA 0012 airfoil type.

INTRODUCTION

Amidst of high demand of energy, the world is seeking alternative energy sources. Wind alone can fulfil most of the energy requirement of the world by its efficient conversion in to energy. On efficiency measurement, Horizontal Axis Wind Turbines (HAWT) is the popular to the researchers, but it works best in places where the wind is not disturbed and has high wind power. The inherent advantage of facing the wind direction, simplistic design, cheap technology for construction, lower wind start-up speeds, easier maintenance, and are relatively quiet is turning the focus to Vertical Axis Wind Turbine (VAWT). The low wind speed and non-smooth wind flow regions are attracted for these machines. VAWTs come in two varieties, Savonius and Darrieus Rotor (Giromill). Savonius turbine is the simplest form of VAWT and operation is based on the difference of the drag force on its blades. In general, VAWT is driven by the two types of forces of wind, drag and lift forces. Savonius rotor is the simplest kind of VAWTs is a drag-type configuration and a bit complex type is

Darrieus rotor which is a lift-type configuration. The operation of Savonius depends on the difference of drag force when the wind strikes the concave and convex part of the semi-spherical blades. The flow energy utilization of Savonius rotor is lower than that of Darrieus rotor. Hence this type of turbine is generally not used for high-power applications and usually used for wind velocimetry applications [1]. The greatest advantage of a Savonius rotor is its ability to self-start in contrast to other 'Lift type' VAWTs [2]. Recently, some generators with high torque at low rotational speed, suitable for small-scale wind turbines, have been developed, suggesting that Savonius rotors may yet be used to generate electric power [3].

The optimum output from the wind energy is the key investigation and based on that different aerodynamic shapes of the blades are designed. Numerous investigations have been carried out in the past to study the performance characteristics of two and three bladed Savonius rotor. These investigations included wind tunnel tests, field experiments and numerical studies. Blade configurations were studied in wind tunnels to evaluate the effect of aspect ratio, blades overlap and gap, effect of adding end extensions, end plates and shielding.

Gupta et al. [4] investigated the performance of two bladed Savonius turbine with five overlaps of 16.2%, 20%, 25%, 30% & 35%. Among them16.2% overlap condition showed maximum power extraction. The pressure drop across the rotor from upstream to down streams well as, maximum pressure difference across the returning bucket is displayed in the same condition. This indicates the better overall aerodynamic torque and power.

Morshed [5] experimented on three bladed Savonius rotor with overlap ratio (OR) of 0, 0.12 and 0.26 using different Reynolds number (Re). The model with no overlap ratio (OR) showed better torque coefficient (C_q) for lower Re, better power coefficient at higher Re and with the increase of tip speed ratio (TSR).

Biswas et al. [6] conducted the experiment on three bladed Savonius turbine in a sub-sonic wind tunnel with no overlap and for overlap conditions in the range of 16% to 35%. They found out that, at no overlap condition, maximum power factor is 36% without blockage correction at TSR of 0.50, and 28% with blockage correction at TSR of 0.46. With the increase of overlap ratio, the values of power-coefficient (C_p) decreased by including blockage effects. Power coefficients increased with the increase of overlap ratio up to a certain limit but afterwards start decreasing, even the overlap is increased. From this experiment the maximum power coefficient is 47% without blockage correction and 38% with blockage correction at 20% overlap.

Qasim et al. [7] worked with impeller scoop-frame type with movable vanes wind turbine VAWT. The objective is to maximize the drag factor by closing the vanes on convex shape and open when air hit the concave part. Due to movement of vanes for and against of wind, a higher drag factor is worked on the impeller scoop-frame type with movable vanes, and has higher efficiency than flat vanes.

Saha et al. [8] studied the performance of twisted blade with all the tests were carried out in a three-bladed system with blade aspect ratio of 1.83. The study shows there is potential of smooth running, higher efficiency and self-starting capability with twisted blades compared semicircular bladed rotor. For yielding maximum power and better starting characteristics at lower wind velocity, larger twist angle is preferable. The optimum performance is displayed at low airspeeds of λ= 6.5m/s and twist angle of α =15° in terms of starting acceleration and maximum no load speed.

Ghatage et al. [9] have done experiment by changing shape of blade as well as the changing the blade number. They have studied with both regular curved blade and twisted curved blade. The experiment concluded that two blades with twist enhance the efficiency of turbine. In their experiment the two-bladed 30° twisted bladed turbine gave the better power coefficient. It can be concluded that the twisted blade attributes relatively higher drag over the turbine surface.

Ghosh et al. [10] have experimented single- and three-stage modified Savonius rotors, which are extensively tested in an open jet wind tunnel. With the increase in the Reynolds number both the single- and three-stage rotors shows higher coefficient of power. The three-stage rotor showed positive and uniform coefficient of static torque. Here the number of blade also has some effect. The coefficient of static torque differs with the change of blade number in a three-stage rotor.

Kumbernuss et al. [11] studied two-staged Savonius-type turbines with different number of blades, the shape of the blades, the overlap ratio and the phase shift angle. The wind turbine was tested under four different wind speeds of 4m/s, 6m/s, 8m/s and 10m/s. There were three turbines with the overlap ratios of 0, 0.16 and 0.32. Before testing those in an open wind tunnel, the wind turbines were adjusted to the phase shift angles (PSA) of 0, 15, 30, 45 and 60 degrees under different air velocities. The overlap ratio is 0.16 produced the better performance among the three, followed by the 0.32 overlap ratio. At lower air velocities the larger phase shift angles and at higher air velocities smaller phase shift angles will produce better performance of the turbines.

Like Savonius, many experiments have been studied to find the optimum performance of Derriues rotor or Giromill. These investigations included mostly numerical studies and some are simulated in wind tunnel as well as in field. Blade configurations were studied to evaluate the effect of blade shape and angle, blade material, aerodynamic characteristics. Some tried to change the external factors which may improve the starting characteristics of Darrieus rotor.

Howell et al. [12] experimented on small scale Darrieus rotor. A combined experimental study in wind tunnel and computational study was done to find the aerodynamics and performance. In this experiment they have changed wind velocity, tip-speed ratio, solidity and rotor blade surface finish. It has been found that, below a critical wind speed (Reynolds number of 30,000) a smooth rotor surface finish degrades the performance of the turbine. The tests also shows that the both two and three bladed rotor models produces highest performance coefficient, but that the three bladed design did so at a much reduced Tip Speed Ratio. Considering errors and uncertainties in both the CFD simulations and the wind tunnel measurements, computational study displays reasonably good agreement with the experimental measurements. Stronger tip

vortices are created at phases with higher amounts of lift are present.

Qin et al. [13] worked with small size straight bladed Darrieus turbine. They have studied with 2D and 3D simulation highlight strong three dimensional effects including the blade tip losses and the effects of the blade supporting shaft and arms. The dynamic stall study has shown a large difference in instantaneous lift coefficients in the windward and the leeward sides of the VAWT blades. The strong three dimensional effect result in a significant reduction in the wind power extraction rate. Minimizing the three dimensional effects, particularly tip speed ratio may improve the Efficiency of the VAWTs.

Beri and Yao [14] studied to show the effect of camber airfoil for a self-starting Darrieus turbine. For this purpose they have used three bladed NACA 2415 camber airfoil and simulated in different tip speed ratio. The experiment results showed that, camber airfoil have the characteristics of self-starter. Though for same power coefficient the efficiency is less than the non-self-starting airfoils.

Hwang et al. [15] researched to find the performance improvement of the straight-bladed Darrieus rotor. The cycloidal blade system and the individual active blade control system are adopted to improve the performance of the power generation system, which consists of several blades rotating about axis in parallel direction. Aerodynamic analysis is carried out by changing pitch angle and phase angle. They have come to a conclusion that, optimal pitch angle variation is obtained by maximizing the tangential force in each rotating blade at the specific rotating position. By this method, the power output is improved about 60% comparing with VAWT using fixed pitch and symmetric airfoil

Hameed and Afaq [16] designed a straight symmetrical blade for a small scale Darrieus rotor using beam theories. They changed the design parameters of the blade like solidity, aspect ratio, pressure coefficient for experiment purpose. Then the blade design was analysed at extreme wind conditions where maximum values of deflection and bending stresses were determined at peak values of aerodynamic and centrifugal forces. It has been concluded that keeping the maximum stresses and deflection within acceptable range, the wall thickness of the blade can be optimized by reducing weight of the blade.

Gupta and Biswas [17] made a comparative study of the performances of twisted two-bladed and three-bladed airfoil shaped H-Darrieus turbine. The models of the turbines were designed, fabricated, and tested in a subsonic wind tunnel. Both power and torque coefficient of the two-bladed turbine were higher than the three-bladed turbine.

Gupta and Biswas [18] further analysed the performance of a three-bladed straight chord H-Darrieus turbine with 30 degree twist at blade tip through 2D steady-state CFD simulation. The standard k-ε turbulence model with enhanced wall condition was used. It was found that pressure and velocity decreased from upstream side to downstream side of the turbine results in increase to overall lift for the turbine. The maximum power coefficient of 0.108 was obtained at tip speed ratio of 2.176. They have also concluded that, twisted shape of the blade facing the upstream flow would improve the performance of the turbine.

Armstrong et al. [19] investigated the aerodynamics of a high solidity Darrieus rotor through wind tunnel tests. This experiment was limited at Re >500,000 for full size operating turbine. Straight blades and canted blade showed different flow separation behavior. Canted blades experiencing less flow reversal on their upwind pass, and recovering attached flow before $\theta = 180^0$. Much less flow separation was noted relative to the straight blades at the same blade speed ratios even for the peak blade ratio $\lambda = 2.1$. Canted blades increased the power and reduced the blade speed ratio at which peak power occurred. The addition of fences, which acted to impede span wise flow on the swept blades, reduced the blade speed ratio at peak power to about $\lambda = 1.9$, presumably with a flow that is more similar to the straight blade case.

Castelli et al. [20] presented a model for the evaluation of aerodynamic and inertial contributions to a vertical axis wind turbine (VAWT) blade deformation. Solid modeling software, capable of generating the desired blade geometry depending on the design geometric parameters, is linked to a finite volume Computational Fluid Dynamic (CFD) code for the calculation of rotor performance and to a Finite Element Method (FEM) code for the structural design analysis of rotor blades. Flow field characteristics are investigated for a constant unperturbed free-stream wind velocity of 9 m/s, determining the torque coefficient generated from the three blades. The computed inertial contribution to blade deformation resulted quite higher with respect to the aerodynamic one for all the analysed blade shell thicknesses. Both inertial and aerodynamic displacements resulted higher at blade trailing edge than at leading edge. They have suggested for further investigation on the influence of this blade section deformation on the aerodynamic performance.

Carrigan et al. [21] had the objective to introduce and demonstrate a fully automated process for optimizing the airfoil cross-section of a vertical-axis wind turbine. The objective is to maximize the torque while enforcing typical wind turbine design constraints such as tip speed ratio, solidity, and blade profile. This work successfully demonstrated a fully automated process for optimizing the airfoil cross-section of a VAWT. As this experiment was not an extensive study, so they have suggested further research and development.

Currently many researchers have been investigating the characteristics to improve the efficiency of different VAWTs and find out the optimum design. Numerical and Experimental research is going on to find the optimum number and shape of blades, overlap ratio and number of layers for Savonius rotor. On the other hand investigation is going on the aerodynamic behavior of the blades of Darrieus rotor to increase the value of starting torque. Finite Element simulation of the structural stress of the VAWT's overall model, blades' material, or stability analysis has not been extensively studied, if studied at all. So the purpose of this study is to perform a finite element static stress analysis to develop structurally stable and relatively efficient vertical axis wind turbine (VAWT) model design. For the finite element simulation, three different VAWT models such as conventional Savonius rotor, Helical Savonius rotor, and the Giromill type VAWT were considered. The ANSYS

FLUENT, a finite element based computational fluid dynamics solver, is adopted to obtain the pressure distributions on the Savonius type models and the lift force for the Giromill model. Each of the VAWTs is tested in ANSYS static structural modeler with three different types of materials such as aluminum alloy, stainless steel, and PVC. Also the Giromill turbine model is tested using two different types of airfoils that have two different lift coefficients. Comparison of the symmetric NACA 0012 and NACA 0714 airfoils of unit chord were chosen for the analysis of the Giromill model design. The goal of the numerical simulation was to determine the location of maximum stress concentrations and total deformation of the blades of each model to determine the structural stability improvement and efficient design of the VAWT models.

NOMENCLATURE

Symbol	Explanation
A	Rotor area
D	Overall rotor diameter
d	Blade diameter
H	Rotor height
a	Overlap distance between two adjacent blades
V	Wind velocity, m/s
N	Revolution per minute
ν	Kinematic viscosity, m^2/s
ρ	Air density, kg/m^3
OR	Overlap ratio: ratio of overlap distance between two adjacent blades and rotor diameter (OR = a/D)
AR	Aspect ratio
ω	Angular velocity, rad/sec
Re	Reynolds Number
λ or, TSR	Tip speed ratio
T	Torque
P	Power
Δp	Pressure difference
F_l	Lift force
F_n	Normal drag force
F_t	Tangential drag force
C_n	Normal drag coefficient
C_t	Tangential drag coefficient
C_q	Torque Coefficient
C_p	Power Coefficient
C_l	Lift Coefficient
η	Efficiency

METHODOLOGY

Model Preparation

Savonius, Helical Savonius, and Giromill VAWTs geometric models were drawn using SolidWorks. The Giromill airfoils were chosen to be the common NACA 0012 and NACA 0714 symmetric profiles. The airfoils were built as separate parts and attached to the frame of the Giromill as an assembly in order to quickly change the airfoils for analysis. The Savonius types were also built as an assembly. Similar scale was used for each of the models to allow for easier interpretation and comparison of final results between each of the blade types. For the Savonius types ANSYS FLUENT is used in order to accurately model pressure distribution. The FLUENT software contains the capabilities needed to model turbulence, heat transfer, and air flow. To do this an enclosure was made around the turbine models and a flow of air was implemented at the inlet with a velocity of 12 m/s which is the optimum condition for Savonius type turbines. Once the pressure difference was found it was taken into ANSYS static structural for simulation. The Giromill did not have to put into FLUENT because the lift force is calculated using formula and the values for the airfoils geometry were taken from an online database. The optimum wind speed for the Giromill was taken to be 13m/s. Table 1 lists the starting conditions for the two types of Savonius wind turbine models. The pressure difference for each type was dependent on the geometry of the blade.

Table 1: Initial conditions for ANSYS Static Structural

Blade Type	Wind speed(m/s)	Min. Pressure(Pa)	Max Pressure(Pa)
Savonius	12	-105.06	158.72
Helical Savonius	12	-433.35	228.36

Mesh and Element Selection

In order to determine the best mesh to use, several tests were performed. Three different methods were used when determining the mesh, the automatic method, tetrahedron method, and the hex dominant method. Each of these meshes were tested for coarse, medium, and fine meshes and compared to see which mesh converged faster with the least number of elements. As can be seen in table 2 the automatic method results converged with the fewest number of elements which lead to reduced simulation time. The similar steps were followed for the meshing of the Helical Savonius model. The automatic method selected the SOLID186 element type which is a 3D 20 nodes that exhibit quadratic behavior. The same element was used for the Helical Savonius model.

For the NACA 0012 and NACA 0714 airfoil Giromill the mesh had to be more complex due to the complex nature of airfoil profiles. In order to receive the appropriate mesh the element type SOLID187 was used, which is a 3-D 10 node based element used for the tetrahedron method. The airfoils went through 2 stages of refinement. Converged solutions were received with this mesh type. The NACA 0012 airfoil Giromill model mesh consisted of using a tetrahedron method with a patch independent algorithm. The minimum size limit was a user defined input to be 25 mm. The relevance center was set using medium and fine settings. Through trial and error of obtaining a usable mesh, the patch independent method remained the only option in being able to generate the mesh type. This method uses geometry to associate the boundary faces of the mesh to the regions of interest.

RESULTS AND DISCUSSION

Three different vertical axis wind turbines have been considered in this study. The Von-Mises equivalent stress and total deformation on the blades have been determined using the finite element technique for these three types of VAWTs. Three types of materials have been chosen for this analysis of the VAWTs models.

TWO BLADED SAVONIUS VAWT MODELS

Once the mesh was decided on and the static conditions were found, the blades were put under these loads on ANSYS static structural and tested for the equivalent Von-Mises stresses and the total deformation. Three different materials were used for Savonius turbine model preparation and tested. These are Aluminum Alloy, Stainless Steel, and Polyvinyl Chloride (PVC).

Mesh dependence on the equivalent stress distribution and total deformation distribution on the two blades of the Savonius wind turbine model have been observed. For this purpose three mesh generating methods have been considered. Equivalent Von-Mises stress and total deformation have been determined using three types of meshes for all three methods which are summarized in Table 2.

Table 2: Aluminum alloy Savonius turbine model results using three mesh types and three meshing methods

Mesh Type	No. of Nodes	No. of Elements	Max. Total Deformation (mm)	Max. Equiv. Stress (MPa)
Automatic method				
Coarse	8197	1078	1.9795	2.3632
Medium	26712	3638	1.9811	2.4678
Fine	60531	9484	1.9838	2.5026
Tetrahedral Method				
Coarse	9156	4159	1.0929	2.8595
Medium	32380	14845	1.9508	2.5779
Fine	56670	27286	1.9718	2.5484
Hex Dominant Method				
Coarse	25019	8716	1.7132	3.1895
Medium	41010	13680	1.9570	2.6136
Fine	61502	19446	1.9662	2.5620

Figure 1 shows (Appendix A) the stress distribution and total deformation distribution along the two blades using fine mesh for automatic mesh generating method. Similarly, Figure 2 and Figure 3 show (Appendix A) the equivalent stress distribution and total deformation distribution for tetrahedral and Hex Dominant mesh generating methods respectively. In all these three cases Aluminum alloy has been considered as blade material. By comparing these three meshing methods results from Table 2 and Figures 1, 2, and 3, automatic fine mesh method has been considered as the optimum method for the equivalent stress and total deformation calculation. So, automatic fine meshing has been used for all simulation calculations for all three materials of two types Savonius turbines.

To see the effect of material dependence, the equivalent stress distribution and total deformation distribution on the two blades of the Savonius wind turbine model have been observed by changing the blade materials. Figures 4, 5 and 6 show (Appendix A) the total deformation and the equivalent stress distribution along blades of the Savonius wind turbine models using Aluminum alloy, stainless steel and PVC respectively. Equivalent Von-Mises stress and total deformation have been determined using three different types of materials which are summarized in Table 3. The number of nodes and elements remained the same because the geometry did not change although the material has changed.

Table 3: Savonius wind turbine model equivalent stress and total deformation results using three different materials

Material	No. of Nodes	No. of Elements	Max. Total defor. (mm)	Max. Equiv. Stress (MPa)
Aluminum alloy	60531	9484	1.9838	2.5026
Stainless Steel	60531	9484	0.73956	2.5103
PVC	60531	9484	39.465	2.4578

For the two bladed Savonius turbine the mesh was simple to obtain because of the simple geometry. The SOLID186 element type has been selected which is a 3-D 20-node element that is quadrilateral in nature. Blades of this regular Savonius turbine had maximum total deformation of 0.739 mm, 1.984 mm, and 39.47 mm for the stainless steel, aluminum alloy and the PVC respectively. This is because stainless steel is a stronger and more rigid material than the other two materials. The maximum equivalent stresses were found to be 2.51MPa, 2.50MPa, and 2.46MPa in the same order of material selection.

HELICAL TYPE SAVONIUS VAWT MODELS

The next turbine type that has been considered is the Helical Savonius VAWT. To observe the effect of material dependence on this new design of Savonius model geometry, the equivalent stress distribution and total deformation distribution on the two blades of the Helical Savonius wind turbine model have been determined by changing the blade materials. Figures 7, 8, and 9 show (Appendix B) the total deformation and the equivalent stress distribution along blades of the Helical Savonius wind turbine models using Aluminum alloy, stainless steel and PVC respectively. Equivalent Von-Mises stress and total deformation of the Helical Savonius Wind turbine model have been determined using three different types of materials which are summarized in Table 4. The number of nodes and elements remained the same because the geometry did not change although the material has changed.

Table 4: Helical Savonius wind turbine model equivalent stress and total deformation results using three different materials

Material	No. of Nodes	No. of Elements	Max Total def. (mm)	Max. Equiv. Stress (MPa)
Aluminum alloy	77411	10750	5.3127	12.426
Stainless Steel	77411	10750	1.9802	12.413
PVC	77411	10750	104.37	12.997

The Helical Savonius wind turbine blades show that the results follow the order from least deformation to most deformation for stainless steel, aluminum alloy, and the PVC materials respectively. The maximum total deformations found in this order are 1.98 mm, 5.31mm, and 104.37mm. It seems that PVC had a hard time handling the wind speed that is rated for the other two types of blades. It was important to note that this deformation also includes the rotation of the blades and not necessarily damage to the turbine. Again the stresses for the Helical Savonius blades were similar to each other for each material. The stainless steel, aluminum alloy, and the PVC were found to have maximum equivalent stresses are 12.43MPa, 12.41MPa, and 12.99MPa respectively.

GIROMILL VAWT MODELS

The third type of VAWT model considered in this study is the Giromill with the NACA 0714 airfoil profile. The lift coefficient of this profile is $C_l = 1.435$. A schematic view of the cross section of a Giromill VAWT is shown in Figure 10 (Appendix C) which shows the direction of drag and lift force direction on the airfoils. To observe the effect of material dependence on the design of Giromill model geometry, the equivalent stress distribution and total deformation distribution on the four blades of the Giromill wind turbine model have been determined by changing the blade materials. Figures 11 and 12 show (Appendix C) the total deformation and the equivalent stress distribution along blades of the Giromill wind turbine with the NACA 0714 airfoil profile models using Aluminum Alloy, and Stainless Steel respectively. Von-Mises equivalent stress and total deformation of the NACA 0714 Giromill wind turbine model have been determined using two different types of materials which are summarized in Table 5. The number of nodes and elements remained the same because the geometry did not change although the material has changed.

Table 5: NACA 0714 Giromill wind turbine model equivalent stress and total deformation results using two different materials

Material	No. of Nodes	No. of Element	Max. Total def. (mm)	Max. Equiv. Stress (MPa)
Aluminum alloy	75436	36357	16.642	230.87
Stainless Steel	75436	36357	10.643	408.21

Another type of airfoil shape has been considered for the structural analysis of Giromill is NACA 0012 airfoil. The lift coefficient of this is $C_l = 0.97$. The equivalent stress distribution and total deformation distribution on the four blades of the Giromill wind turbine model have been determined by changing the blade materials. Figures 13 and 14 show (Appendix C) that the total deformation and the equivalent stress distribution along blades of the Giromill wind turbine with the NACA 0012 airfoil profile models using Aluminum Alloy, and Stainless Steel respectively.

The testing of the NACA 0714 airfoil profile was much more consistent than that of the NACA 0012. The lift force of the NACA 0714 was greater than that of the NACA 0012. PVC could not handle being run in ANSYS and actually the model was compressed during the simulation. The aluminum alloy had maximum total deformation of 16.642 mm and an equivalent stress of 230.87 MPa. Whereas, the stainless steel had maximum total deformation of 10.643 mm and maximum equivalent stress of 408.21 MPa. As mentioned earlier SOLID187 3-D 10-node was the best element type for the NASA 0714 blade type.

While gathering equivalent stress and deflection data for the NACA 0012 Airfoil Giromill, many problems occurred while attempting to generate the mesh. The conventional Automatic Method and Hexagonal Method were not able to be used in generating mesh due to errors initialized in ANSYS. As mentioned in the procedure portion of this report, the tetrahedron method with a patch independent method was the only method that allowed a mesh to be generated. The results for this mesh include the following elements used: SOLID187, CONTA174, TARGE170, SURF154, and COMBIN14. SOLID187, a 10-node element, was the ideal element in this case due to the geometry setup for the blades designed in Solidworks. Concerning the analysis on the materials used for this Giromill: Aluminum alloy displayed the maximum total deformation of 0.067 mm with a maximum equivalent stress of 5.88MPa. Stainless steel had a maximum total deformation of 0.00018 mm and maximum equivalent stress of 5.79 MPa.

CONCLUSION

Three different types of VAWT models such as conventional Savonius rotor, Helical Savonius rotor, and the Giromill type VAWT were analysed using finite element methods. The following findings can be made from this finite element simulation for these three different VAWT models:

1. For the two bladed Savonius VAWT model, stainless steel model gives the least maximum total deformation compared to the other two models made of aluminum alloy and PVC.
2. For the two bladed Savonius VAWT model, the maximum equivalent stress values are almost same for all three types of materials used for models fabrication.
3. Similar trend can be observed for the Helical Savonius VAWT model in regard to the maximum total deformation of the models made of three different materials although the corresponding values of the

deformations are more in these cases compared to the regular Savonius cases.

4. The maximum equivalent stress values are also almost same for all three Helical Savonius models made of three different materials. But the corresponding values are more for all three cases compared to the regular Savonius models.
5. Two types of airfoils NACA 0714 and NACA 0012 have been used for the Giromill type VAWT models; in these two types airfoil NACA 0714 type airfoil gives consistent results both for maximum total deformation and maximum equivalent stress. In these cases for Giromill type VAWT models testing materials used were stainless steel and aluminum alloy in which stainless steel gives least total deformation but more maximum equivalent stress compared to model made of aluminum alloy.

REFERENCES

[1] Islam, M., DSK Ting, and A. Fartaj. "Aerodynamic models for Darrieus-type straight bladed vertical axis wind turbines." *Renewable and Sustainable Energy Reviews*, no. 12 (2008): 1087–109.

[2] Mohamed, MH, G Janiga, E. Pap, and D. Thevenin. "Optimal blade shape of a modified Savonius turbine using an obstacle shielding the returning blade." *Energy Conversion and Management*, no. 52 (2011): 236–42.

[3] Hayashi, T., Y. Li, Y. Hara, and Y. Suzuki. "Wind Tunnel Test on a Three Stage out phase Savonius Rotor." *Proceeding of European Wind Energy Conference and Exhibition.* London, England, 2004.

[4] Gupta, R., R. Das, R. Gautam, and S.S. Deka. "CFD Analysis of a Two bucket Savonius Rotor for Various Overlap Conditions." *ISESCO Journal of Science and Technology* 8-13 (May 2012): 67-74.

[5] Morshed, Khandakar N. *Experimental and numerical investigations on aerodynamic characteristics of savonius wind turbine with various overlap ratios.* Statesboro: Georgia Southern University, 2010.

[6] Biswas, A., R. Gupta, and K.K. Sharma. "Experimental Investigation of Overlap and Blockage." *Wind Engineering* 31-5 (2007): 363–368.

[7] Qasim, A.Y., R. Usubamatov, and Z.M. Zain. "Investagation and Design Impeller Type Vertical Axis Wind Turbine." *Australian Journal of Basic and Applied Sciences* 5(12) (2011): 121-126.

[8] Saha, U.K., S. Thotla, and D. Maity. "Optimum design configuration of Savonius rotor through wind tunnel experiments." *Journal of Wind Engineering and Industrial Aerodynamics*, no. 96 (2008): 1359– 1375.

[9] Ghatage, Swapnil V., and Jyeshtharaj B. Joshi. "Optimisation of Vertical Axis Wind Turbine:CFD Simulations and Experimental Measurements." *The Canadian Journal of Chemical Engineering* 90 (2012): 1186-1201.

[10] Ghosh, P., M. A. Kamoji, S. B. Kedare, and S. V. Prabhu. "Model Testing of Single and Three-stage Modified Savonius Rotors and Viability Study of Modified Savonius Pump Rotor Systems." *International Journal of Green Energy*, no. 6 (2009): 22–41.

[11] Kumbernuss, J., J. Chen, H.X. Yang, and L. Lu. "Investigation into the relationship of the overlap ratio and shift angle of double stage three bladed vertical axis wind turbine (VAWT)." *Journal of Wind Engineering and Industrial Aerodynamics*, no. 107 (2012): 57-75.

[12] Howell, Robert, Ning Qin, Jonathan Edwards, and Naveed Durrani. "Wind tunnel and numerical study of a small vertical axis wind turbine." *Renewable Energy* 35 (2010): 412-422.

[13] Qin, Ning, Robert Howell, Naveed Durrani, Kenichi Hamada, and Tomos Smith. "Unsteady Flow Simulation and Dynamic Stall Behaviour of Vertical Axis Wind Turbine Blades." *Wind Engineering* 35-4 (2011): 511-527.

[14] Beri, H., and Y. Yao. "Effect of Camber Airfoil on Self Starting of Vertical Axis Wind Turbine." *Journal of Environmental Science and Technology* 4-3 (2011): 302-312.

[15] Hwang, In Seong, Seung Yong Min, In Oh Jeong, Yun Han Lee, and Seung Jo Kim. *Efficiency Improvement of a New Vertical Axis Wind Turbine by Individual Active Control of Blade Motion.* Brain Korea 21 Project, Seoul, Korea: Seoul National University, 2012.

[16] Hameed, M. Saqib, and S.Kamran Afaq. "Design and analysis of a straight bladed vertical axis wind turbine blade using analytical and numerical techniques." *Ocean Engineering* 57 (2012): 248-255.

[17] Gupta, Rajat, and Agnimitra Biswas. "CFD analysis of a three-bladed straight chord H-darrieus turbine with 30 degree twist at blade tip." *Proceedings of the ASME 2011 5th International Conference on Energy Sustainability.* Washington, DC, USA, 2011.

[18] Gupta, Rajat, and Agnimitra Biswas. "Comparative study of the performances of twisted two-bladed and three-bladed airfoil shaped H-Darrieus turbines by computational and experimental methods." *International Journal of Renewable Energy Technology* 2-4 (2011): 425-445.

[19] Armstrong, Shawn, Andrzej Fiedler, and Stephen Tullis. "Flow separation on a high Reynolds number, high solidity vertical axis wind turbine with straight and canted blades and canted blades with fences." *Renewable Energy* 41 (2012): 13-22.

[20] Castelli, Marco Raciti, Andrea Dal Monte, Marino Quaresimin, and Ernesto Benini. "Numerical evaluation of aerodynamic and inertial contributions to Darrieus wind turbine blade deformation." *Renewable Energy* 51 (2013): 101-112.

[21] Carrigan, Travis J., Brian H. Dennis, Zhen X. Han, and Bo P. Wang. "Aerodynamic Shape Optimization of a Vertical-AxisWind Turbine Using Differential Evolution." *International Scholarly Research Network ISRN Renewable Energy*, 2012.

APPENDIX A:

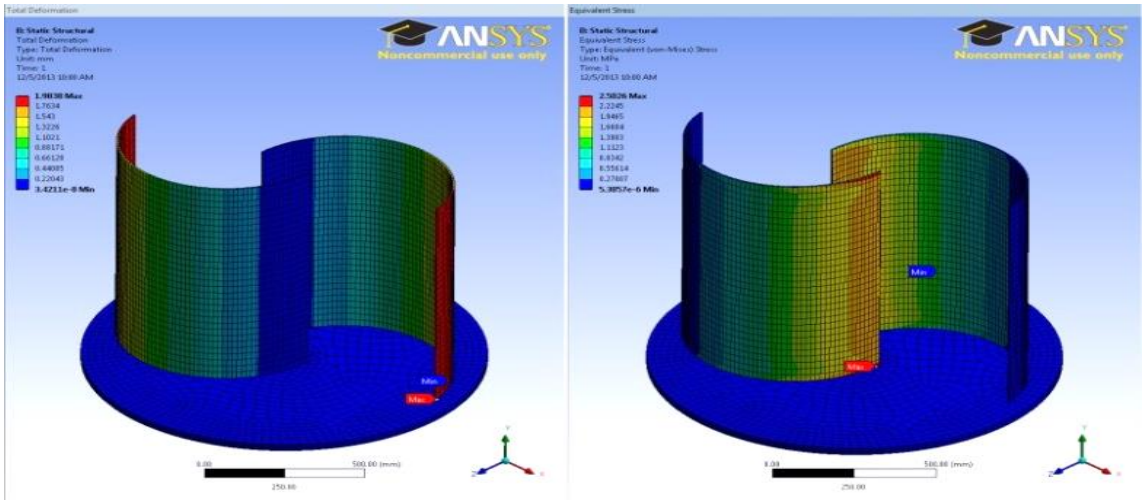

(a) **(b)**

Figure 1 (a) Total deformation along blades, and (b) equivalent stress distribution along blades using automatic fine mesh.

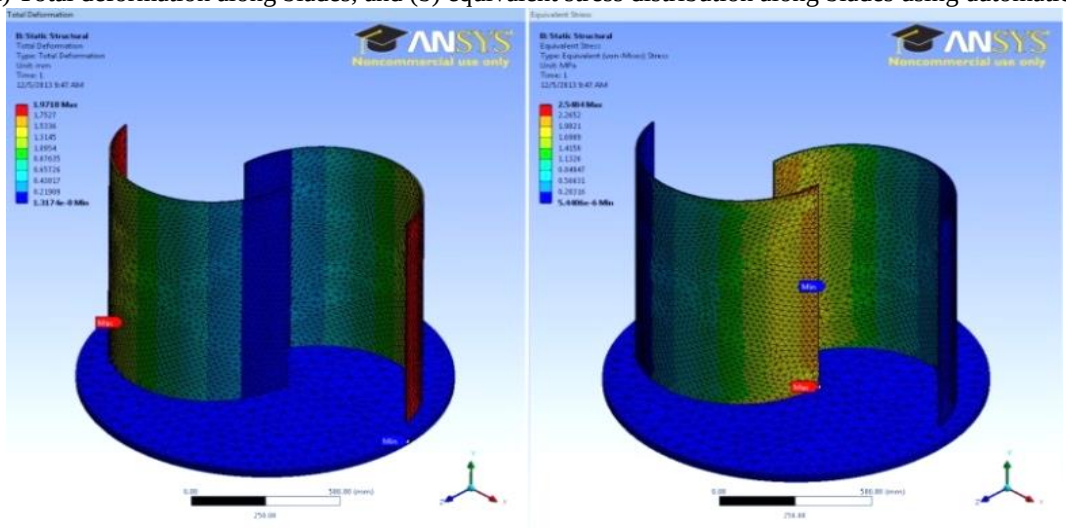

(a) **(b)**

Figure 2 (a) Total deformation along blades, and (b) equivalent stress distribution along blades using tetrahedron fine mesh.

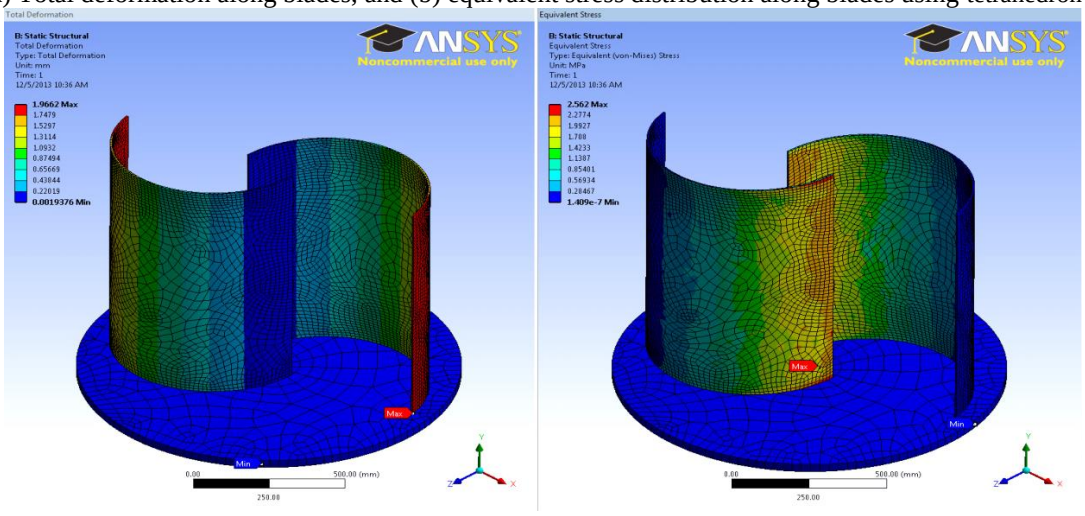

(a) **(b)**

Figure 3 (a) Total deformation along blades, and (b) equivalent stress distribution along blades using hex dominant fine mesh.

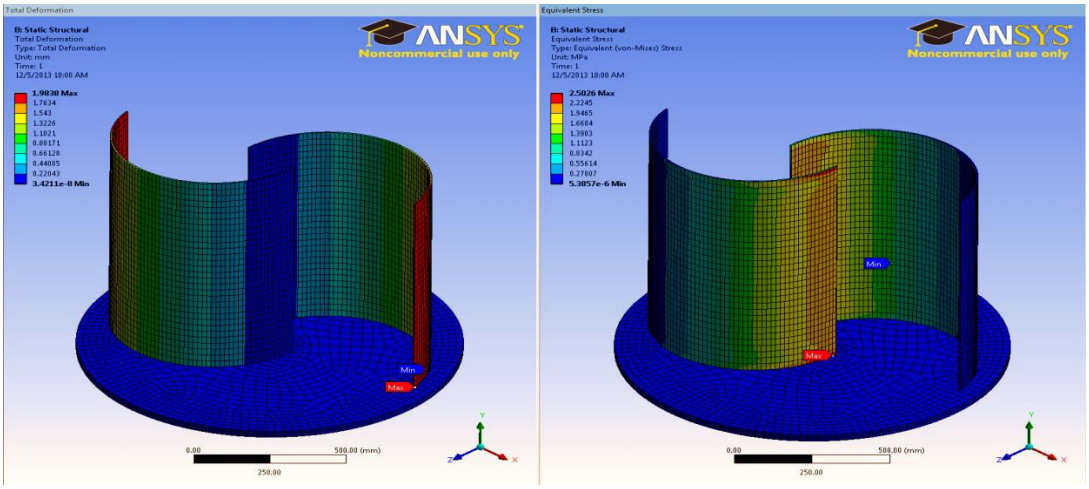

(a) **(b)**

Figure 4 (a) Total deformation along blades, and (b) equivalent stress distribution along blades using Aluminum alloy.

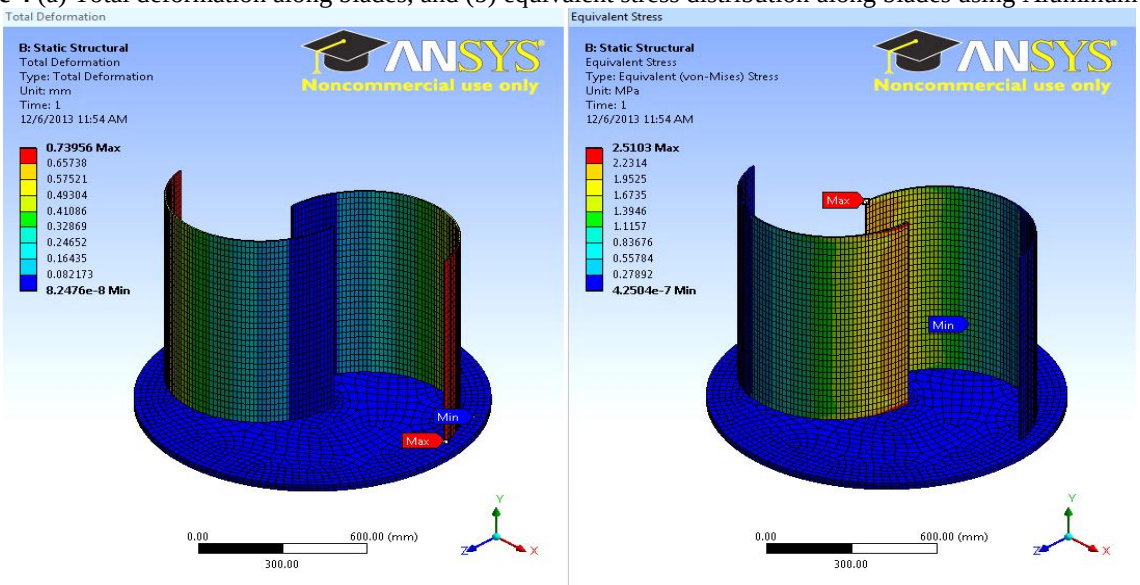

(a) **(b)**

Figure 5 (a) Total deformation along blades, and (b) equivalent stress distribution along blades using Stainless Steel.

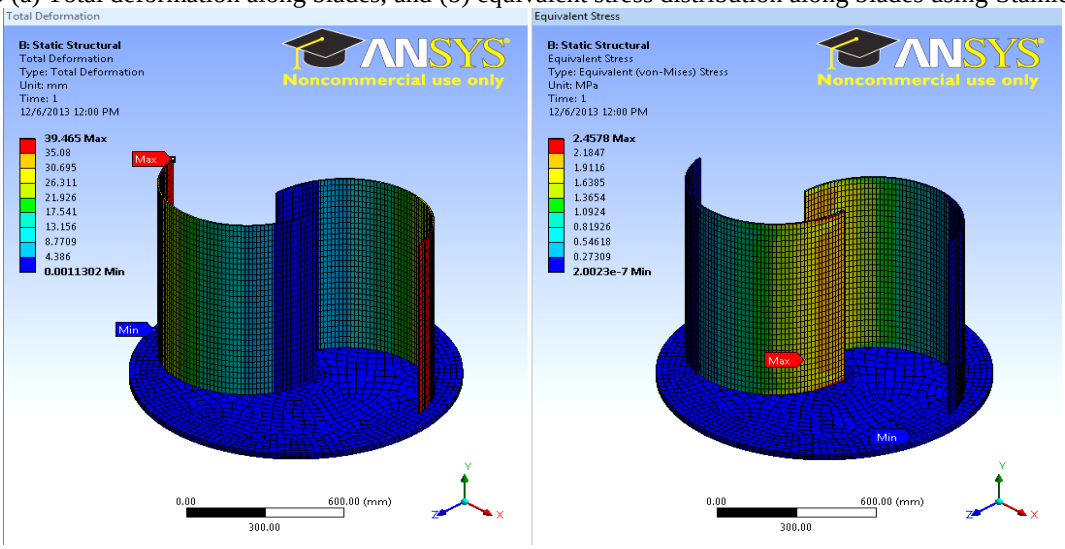

(a) **(b)**

Figure 6 (a) Total deformation along blades, and (b) equivalent stress distribution along blades using PVC.

APPENDIX B:

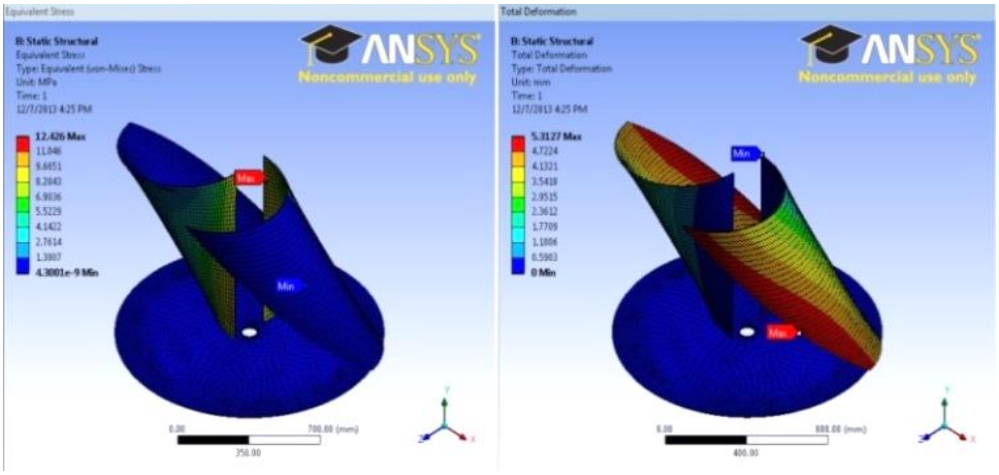

(a) **(b)**

Figure 7 (a) Equivalent stress distribution along blades, and (b) Total deformation along blades using Aluminum alloy.

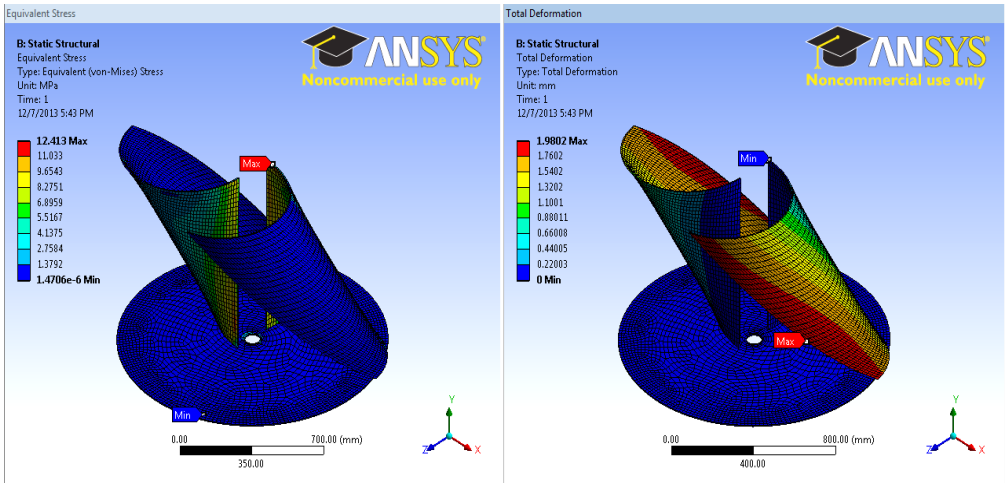

(a) **(b)**

Figure 8 (a) Equivalent stress distribution along blades, and (b) Total deformation along blades using Stainless Steel.

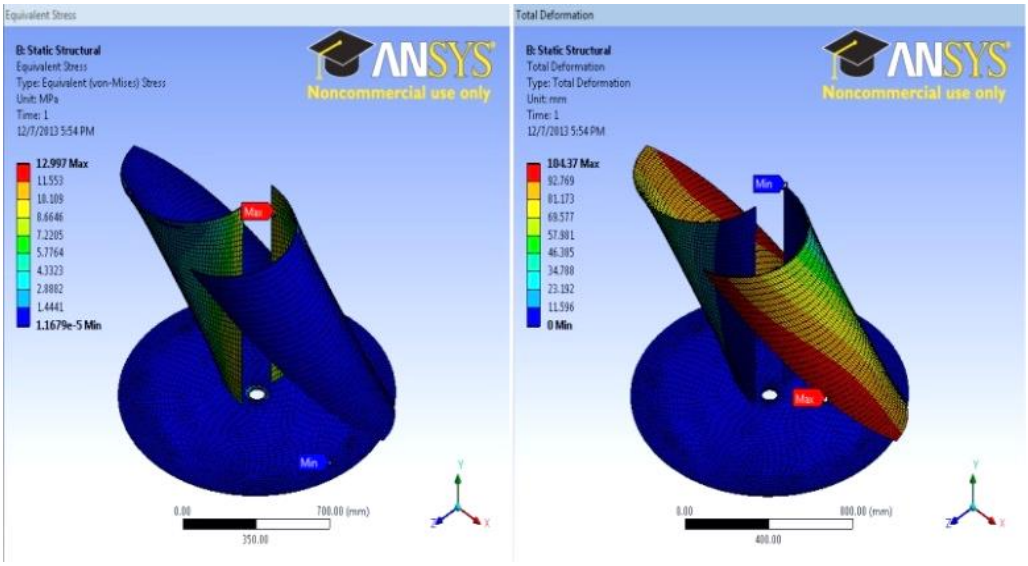

(a) **(b)**

Figure 9 (a) Equivalent stress distribution along blades, and (b) Total deformation along blades using PVC.

APPENDIX C:

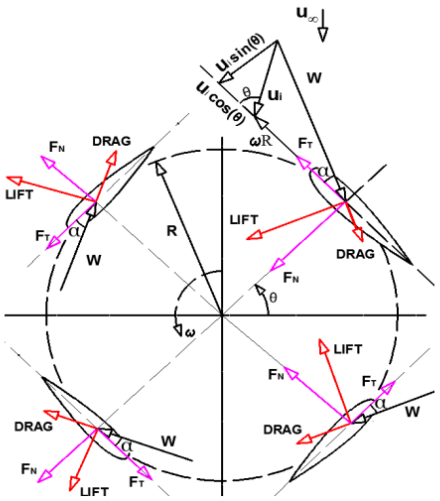

Figure 10 Schematic diagram of the cross section of the Giromill VAWT model showing Lift and Drag forces direction.

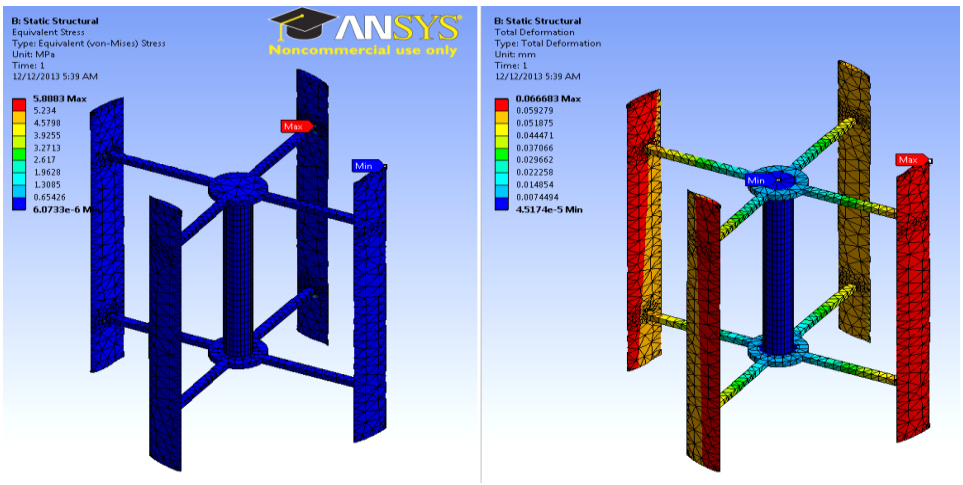

(a) **(b)**

Figure 11 (a) Equivalent stress distribution along blades, and (b) Total deformation along blades using Aluminum alloy.

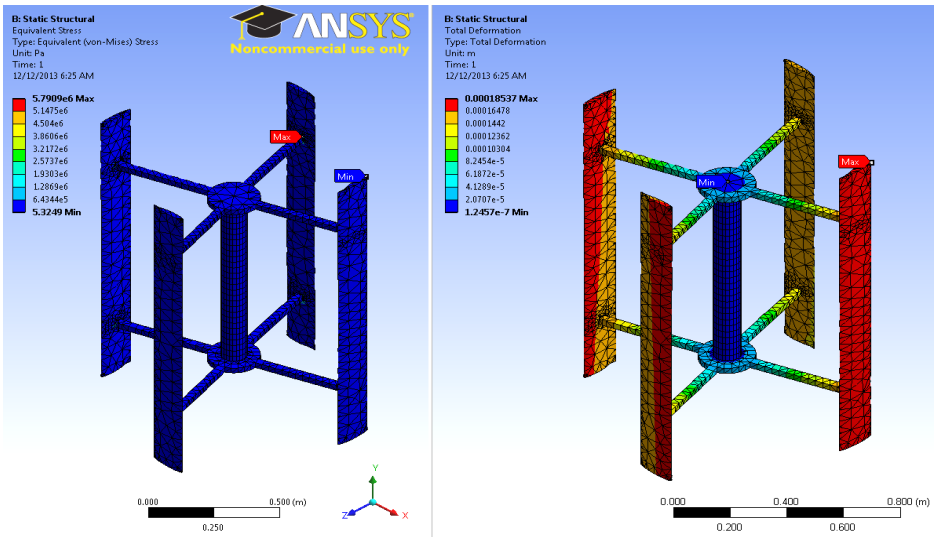

(a) **(b)**

Figure 12 (a) Equivalent stress distribution along blades, and (b) Total deformation along blades using Stainless Steel.

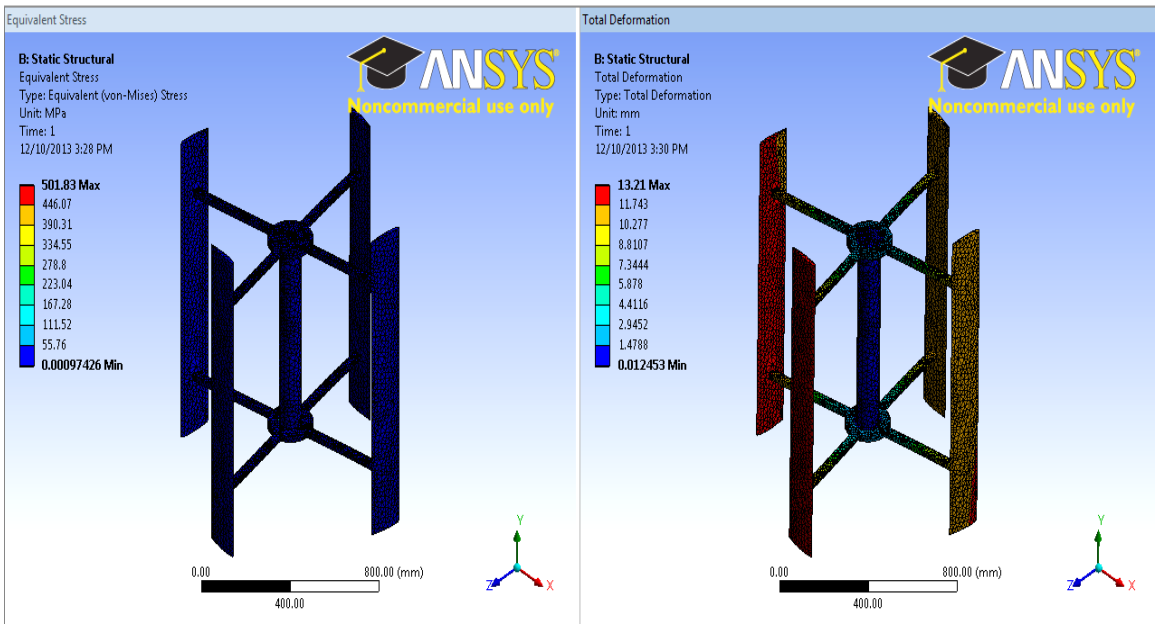

(a) **(b)**

Figure 13 (a) Equivalent stress distribution along blades, and (b) Total deformation along blades using Aluminum alloy.

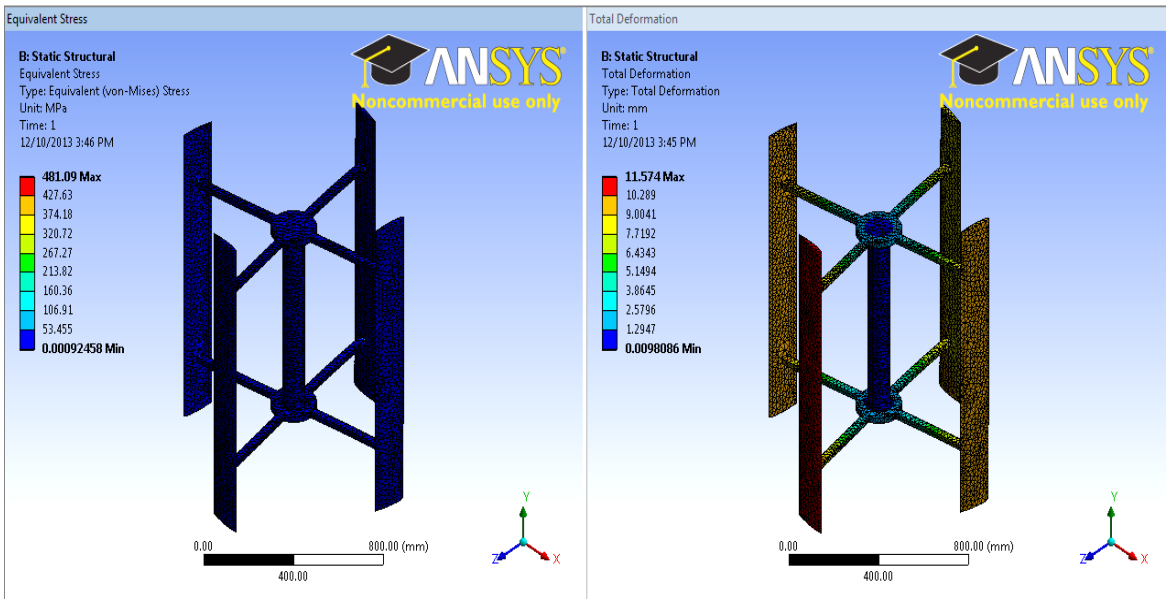

(a) **(b)**

Figure 14 (a) Equivalent stress distribution along blades, and (b) Total deformation along blades using Stainless Steel.